Synthesis, Properties and Crystal Structures of Iron-(II) and -(III) Complexes of 2,2′:6′,2″:6″,2‴-Quaterpyridine†

Chi-Ming Che,[*,a] **Chin-Wing Chan,**[a] **San-Ming Yang,**[a] **Chun-Xiao Guo,**[a] **Chung-Yuan Lee**[b] **and Shie-Ming Peng**[b]

[a] *Department of Chemistry, The University of Hong Kong, Pokfulam Road, Hong Kong*

[b] *Department of Chemistry, National Taiwan University, Taipei, Taiwan*

Several iron complexes of 2,2′:6′,2″:6″,2‴-quaterpyridine (L) in di- and tri-valent oxidation states have been prepared, and the structures of $[FeL(OH_2)_2][ClO_4]_2$ **1**, $[\{FeL(ClO_4)\}_2(\mu\text{-}O)]\cdot 8.5H_2O$ **2**·8.5H₂O and $[\{FeL(Cl)\}_2(\mu\text{-}O)][ClO_4]_2\cdot 2H_2O$ **3**·2H₂O, have been determined by X-ray crystal analyses. In each complex, the quaterpyridine ligand is planar. In **2**, the Fe^{II} is seven-co-ordinate with the $[ClO_4]^-$ acting as a bidentate ligand with Fe–O–Fe 155.2(4)°. In **3**, the Fe–O–Fe unit is linear and the Fe–O distance of 1.779(1) Å is considerably shorter than the $Fe–O(OH_2)$ distance of 2.141(5) Å in **1**. The results of molecular orbital calculations revealed that the unoccupied molecular orbitals of **2** and **3** mainly comprise the π^* orbital of L. In **2**, bending of the Fe–O–Fe unit gives rise to a decrease in the antibonding interaction between $Fe(d_{yz})$ and $O(p_y)$ orbitals. Complex **3** is less stable in the spin-paired ($S = 0$) than in open-shell ($S = 1$) state by 49.3 kcal mol⁻¹. This coincides with magnetic susceptibility measurements which show that **3** is paramagnetic with μ_{eff} 1.75 μ_B per iron atom.

Polypyridines are among the most common chelating ligands for transition-metal complexes of photochemical and electrochemical interests.[1] Although the co-ordination chemistry of 2,2′-bipyridine and 2,2′:6′,2″-terpyridine are well documented,[2] related studies on oligomeric pyridines are still in the development stage. Previous studies by Constable *et al.*[3] and Che and co-workers[4] have demonstrated the versatile co-ordinating ability of 2,2′:6′,2″:6″,2‴-quaterpyridine (L), which usually functions as a tetradentate chelating ligand. Iron complexes of quaterpyridine have also been studied extensively by Pispisa and co-workers[5] but their crystal structures have not been reported. Our interests in iron–quaterpyridine complexes stem from previous studies indicating that high-valent Fe=O species are likely to be generated through oxidation of Fe^{II} and/or Fe^{III} by an oxygen atom donor such as H_2O_2 or Bu^tO_2H in the presence of pyridyl ligands.[6] As quaterpyridine is a good chelating ligand, it may be useful for the study of high-valent Fe=O chemistry. In this work, the synthesis and crystal structures of several tetradentate, quaterpyridine iron complexes are reported.

Experimental

Materials.—2,2′:6′,2″:6″,2‴-Quaterpyridine was prepared by literature methods;[3a] $FeCl_3$, $Fe(ClO_4)_2\cdot xH_2O$ and $Fe(ClO_4)_3\cdot xH_2O$ were used as received. Acetonitrile was distilled over $KMnO_4$ followed by CaH_2.

Physical Measurements and Instrumentation.—Infrared spectra were measured on a Nicolet 20 SXC FT-IR spectrometer, and UV/VIS spectra on a Milton Roy Spectronic 3000 spectrophotometer. Elemental analyses were performed at the Shanghai Institute of Organic Chemistry, Chinese Academy of Science and at the Department of Chemistry of National Taiwan University.

X-Ray Crystal Structure Determination.—Crystal data are listed in Table 1. The diffraction data were collected on an Enraf-Nonius CAD4 diffractometer at 298 K (graphite-monochromated Mo-Kα radiation, $\lambda = 0.710\,70$ Å) with the θ–2θ method. The unit-cell dimensions were obtained from a least-squares fit of 25 reflections in the range of $18.56 < 2\theta < 28.10$ and $18.82 < 2\theta < 27.98°$ for **1** and **2** respectively, and 24 reflections in the range of $18.58 < 2\theta < 24.02°$ for **3**. Calculations were carried out with a NRCVAX refinement program.[7] The final agreement factors $R\ [=(\Sigma|F_o - F_c|)/\Sigma|F_o|]$, $R'\{=[\Sigma w(|F_o| - |F_c|)^2/\Sigma w|F_o|_2]^{\frac{1}{2}}\}$ and $S\ \{=[\Sigma w(|F_o - F_c|)^2/(n-p)]^{\frac{1}{2}}\}$ are also listed in Table 1. The atomic coordinates of all non-hydrogen atoms of **1**, **2** and **3** are listed in Tables 2, 3 and 4 respectively, and selected bond distances and angles are given in Table 5.

Additional material available from the Cambridge Crystallographic Data Centre comprises H-atom coordinates, thermal parameters and remaining bond lengths and angles.

Preparations.—$[FeL(OH_2)_2][ClO_4]_2$ **1**. A mixture of $Fe(ClO_4)_2\cdot xH_2O$ (0.1 g) and L (46.5 mg, 0.15 mmol) in acetonitrile (50 cm³) was heated at 70 °C for 15 min. The solution was filtered and concentrated to about 10 cm³. Upon diffusion of diethyl ether into the solution, red needles were obtained in 87% yield (Found: C, 37.8; H, 3.1; N, 8.3. Calc. for $C_{20}H_{18}Cl_2FeN_4O_{10}$: C, 37.15; H, 2.80; N, 8.65). IR (cm⁻¹): 1463m, 1143s, 1111s, 1087s, 775m, 627m. UV/VIS in CH_3CN: [λ_{max}/nm ($10^{-3}\varepsilon$/dm³ mol⁻¹ cm⁻¹)]: 232 (35), 293 (18), 301 (22), 338 (12), 365 (2.9), 515 (0.72); μ_{eff} = 0 μ_B (Evans' method).

$[\{FeL(ClO_4)\}_2(\mu\text{-}O)]$ **2**. A mixture of $Fe(ClO_4)_3\cdot xH_2O$ (0.2 g) and L (0.05 g, 16 mmol) in water–ethanol (20 cm³, 10:1 v/v) was stirred at room temperature for 1 d. Upon standing for several days, reddish brown crystals were obtained, yield 15% (Found: C, 49.9; H, 3.1; N, 11.40. Calc. for $C_{40}H_{28}Cl_2Fe_2N_8O_9$: C, 50.7; H, 2.95; N, 11.85%); μ_{eff} = 0 μ_B (Evans' method).

$[\{FeL(Cl)\}_2(\mu\text{-}O)][ClO_4]_2$ **3**. 2,2′:6′,2″:6″,2‴-Quaterpyridine (0.025 g) in CH_2Cl_2 (25 cm³) was added to an ethanolic solution of $FeCl_3$ (0.013 g in 10 cm³). The mixture was refluxed for 2 d. Upon additon of $LiClO_4$ to the filtrate, a yellow-orange

---

† *Supplementary data available:* see Instructions for Authors, *J. Chem. Soc., Dalton Trans.*, 1995, Issue 1, pp. xxv–xxx.

Non-SI units employed: $\mu_B \approx 9.274\,02 \times 10^{-24}$ J T⁻¹, cal ≈ 4.184 J.

Table 1 Crystallographic data

Complex	**1**	**2**·8.5H_2O	**3**·2H_2O
Formula	$C_{20}H_{18}Cl_2FeN_4O_{10}$	$C_{40}HCl_2Fe_2N_8O_{17.5}$	$C_{40}H_{32}Cl_4Fe_2N_8O_{11}$
M	601.28	1100.34	1054.54
Crystal dimensions/mm	0.30 × 0.35 × 0.50	0.20 × 0.20 × 0.25	0.30 × 0.25 × 0.30
Crystal system	Monoclinic	Monoclinic	Monoclinic
Space group	$C2/c$	$P2_1/c$	$C2/m$
a/Å	14.633(5)	11.420(2)	15.553(2)
b/Å	11.134(4)	22.046(4)	13.761(3)
c/Å	15.123(6)	18.348(4)	10.357(1)
β/°	98.84(3)	97.82(2)	103.75(1)
U/Å^3	2435(2)	4576(2)	2153.1(6)
F(000)	1224	1134	1072
Z	4	2	2
D_c/g cm^{-3}	1.64	1.57	1.62
μ/cm^{-1}	8.99	8.16	8.16
$2\theta_{max}$/°	50	45	45
h, k, l	−17 to 17, 0–13, 0–17	−12 to 12, 0–23, 0–19	−16 to 16, 0–14, 0–11
Unique data measured	2129	5970	1476
Unique data used, n	1617 [$I_o \geqslant 2\sigma(I_o)$]	2784 [$I_o \geqslant 2\sigma(I_o)$]	1161 [$I_o \geqslant 2\sigma(I_o)$]
Number of variables, p	169	629	159
Number of atoms	28	97.5	27
R, R' and S	0.063, 0.060, 1.76	0.063, 0.058, 2.50	0.052, 0.052, 3.23
Weighting scheme	Unit weight	$[1/\sigma(F_o)]^2$	$[1/\sigma(F_o)]^2$
ρ/e Å^{-3}	−0.54 to +0.67	−0.44 to +0.62	−0.68 to +0.72

Table 2 Non-hydrogen atomic coordinates with estimated standard deviations (e.s.d.s) for $[FeL(OH_2)_2][ClO_4]$

Atom	x	y	z
Fe	0	0.082 08(12)	1/4
N(1)	−0.065 7(4)	0.151 9(5)	0.119 6(3)
N(2)	−0.041 4(4)	−0.072 2(5)	0.169 5(3)
C(1)	−0.073 7(5)	0.267 7(7)	0.097 9(5)
C(2)	−0.114 1(5)	0.307 1(7)	0.014 6(5)
C(3)	−0.146 8(5)	0.222 9(8)	−0.048 3(5)
C(4)	−0.138 8(5)	0.103 0(7)	−0.028 0(4)
C(5)	−0.097 9(4)	0.068 8(6)	0.057 4(4)
C(6)	−0.086 7(4)	−0.057 7(6)	0.086 2(4)
C(7)	−0.119 0(6)	−0.156 2(7)	0.034 4(5)
C(8)	−0.103 4(6)	−0.268 8(7)	0.070 2(5)
C(9)	−0.056 2(6)	−0.284 5(7)	0.155 3(5)
C(10)	−0.025 7(5)	−0.182 1(6)	0.203 5(4)
O(1)	0.128 9(3)	0.111 6(4)	0.203 1(3)
O(2)	0.670 0(10)	−0.157 1(10)	0.143 8(9)
O(3)	0.590 7(7)	−0.041 2(12)	0.201 5(11)
O(4)	0.723 9(10)	−0.093 1(15)	0.268 5(8)
O(5)	0.721 7(6)	0.028 8(8)	0.161 8(6)
Cl	0.675 24(14)	−0.061 92(18)	0.194 30(13)

solid was obtained. This was dissolved in a minimum amount of MeCN and an equal volume of ethanol added. Slow evaporation of the solvent gave some purple crystals, which were found by X-ray crystal analysis to be $[\{FeL(Cl)\}_2(\mu\text{-}O)][ClO_4]_2$, yield 10% (Found: C, 47.50; H, 2.95; N, 10.80. Calc. for $C_{40}H_{28}Cl_4Fe_2N_8O_9$: C, 47.15; H, 2.75; N, 11.00%). UV/VIS in CH_3CN: [λ_{max}/nm (10^{-3} ε/dm^3 mol^{-1} cm^{-1})]: 286 (34), 296 (33), 349 (28), 386 (17). IR (cm^{-1}): 1595s, 1560m, 1488s, 834s, 735s.

Magnetic Susceptibility Measurements.—The magnetic susceptibilities[8] of complexes **1** and **2** were determined by Evans' method in acetonitrile with tetramethylsilane (tms) as the standard. No splitting of the tms signal was observed. The magnetic susceptibility of **3** was determined by the Faraday method using $HgCo(NCS)_4$ as the calibrant (χ_g = 16.44 × 10^{-6} cm^3 g^{-1}) at 26.5 °C. The mass susceptibility (χ_g) and molar susceptibility (χ_m) of **3** were 1.8958 × 10^{-6} and 0.013 95 × 10^{-3} cm^3 g^{-1} respectively. Diamagnetic corrections for **3** were calculated using Pascal's constants[8] (−301.6 × 10^{-6} cm^3 mol^{-1}). The corrected molar susceptibility of **3**, χ'_m = 2.5520 × 10^{-3} cm^3 g^{-1} and thus the effective magnetic moment is 1.75 μ_B per iron atom.

Molecular Orbital Calculations.—Molecular orbital calculations on **2** and **3** were performed by the complete neglect of differential overlaps (CNDO) method. The parameters used for iron were taken from Clark and Allen,[9] those for other atoms are from Pople and Beveridge.[10] The geometric factors were obtained from the X-ray diffraction studies. The atomic positions were transformed into Cartesian coordinates by taking oxygen atom as the origin (0,0,0) with the x-, y- and z-directions defined as follows: both the y- and z-axis are on the imaginary plane containing the Fe–O–Fe moiety. The Fe–O bond is taken as the z-axis in **3**; for **2**, the z-axis is parallel to the line joining the two Fe atoms. The near frontier orbital energies and compositions of **2** and **3** are summarized in Tables 6 and 7 respectively.

Results and Discussion

The reaction of $FeSO_4$ with L and some of the oxidation chemistry of Fe^{II}–L complexes have been extensively studied by Pispisa and co-workers,[5] but no structural study has been reported. In this work, $[FeL(OH_2)_2]^{2+}$ **1** was prepared by treating $Fe(ClO_4)_2 \cdot xH_2O$ with L in boiling acetonitrile, and isolated as a red perchlorate salt. Its UV/VIS absorption spectrum displays an intense absorption around 300 nm (ε > 10^4 dm^3 mol^{-1} cm^{-1}), which is intraligand in nature. There is also an intense broad absorption band ranging from 400 to 500 nm ($\varepsilon \approx 10^3$ dm^3 mol^{-1} cm^{-1}), which is due to a $Fe^{II} \longrightarrow L$ charge-transfer transition.

The complex gradually undergoes ligand dissociation in acidic or basic solution. However, it is more stable in degassed citrate and/or phosphate buffer solutions ($\approx$0.1 mol dm^{-3}). Our attempt to prepare $[FeL(OH_2)(OH)]^{2+}$ by treating $Fe(ClO_4)_3 \cdot xH_2O$ with 0.1 mol dm^{-3} L in ethanol–water was unsuccessful. Instead, a seven-co-ordinated dinuclear Fe^{II} complex, **2**, was formed. Presumably, ethanol acts as the reductant for the reduction of Fe^{III} to Fe^{II}. In aqueous solutions, complex **2** easily converts to **1**. In fact, the cyclic voltammograms of **1** and **2** in 0.1 mol dm^{-3} CF_3SO_3H are virtually identical. In alcoholic solution and with $FeCl_3$ as the starting material, the yellow-orange $[FeL(Cl)_2]ClO_4$ complex was obtained as the initial

Table 3 Non-hydrogen atomic coordinates with e.s.d.s for $[\{FeL(ClO_4)\}_2(\mu\text{-}O)]$

Atom	*x*	*y*	*z*
Fe(1)	0.951 23(16)	0.659 20(9)	0.110 35(10)
Fe(2)	0.717 52(15)	0.669 48(8)	−0.033 69(10)
Cl(1)	1.094 5(4)	0.601 92(20)	0.223 62(22)
Cl(2)	0.560 3(3)	0.623 95(16)	−0.149 20(19)
O	0.833 2(7)	0.646 9(3)	0.036 5(4)
O(1)	1.001 0(8)	0.574 9(4)	0.165 9(5)
O(2)	1.084 5(8)	0.669 0(4)	0.203 9(5)
O(3)	1.065 8(10)	0.589 5(5)	0.298 3(5)
O(4)	1.214 8(8)	0.580 4(5)	0.217 9(6)
O(5)	0.647 0(7)	0.591 5(4)	−0.095 1(4)
O(6)	0.583 9(7)	0.689 2(4)	−0.127 3(5)
O(7)	0.584 9(8)	0.614 0(4)	−0.224 2(5)
O(8)	0.438 4(7)	0.607 3(4)	−0.142 1(5)
N(1)	1.084 4(8)	0.615 4(4)	0.042 0(5)
N(2)	1.051 5(8)	0.730 4(4)	0.061 3(5)
N(3)	0.890 7(9)	0.748 8(5)	0.142 6(5)
N(4)	0.810 9(8)	0.646 7(5)	0.187 2(6)
N(5)	0.850 5(9)	0.652 6(4)	−0.114 7(5)
N(6)	0.789 0(8)	0.757 4(4)	−0.064 2(5)
N(7)	0.627 5(8)	0.744 5(4)	0.019 4(6)
N(8)	0.587 4(8)	0.631 3(4)	0.036 2(5)
C(1)	1.095 4(11)	0.555 4(6)	0.032 5(7)
C(2)	1.170 7(11)	0.528 8(6)	−0.010 4(7)
C(3)	1.237 3(11)	0.568 1(6)	−0.048 8(7)
C(4)	1.231 1(11)	0.629 2(6)	−0.040 9(7)
C(5)	1.152 2(10)	0.650 1(5)	0.005 3(7)
C(6)	1.136 0(11)	0.716 9(6)	0.019 0(7)
C(7)	1.202 1(12)	0.760 8(6)	−0.012 2(8)
C(8)	1.181 4(13)	0.820 5(6)	0.004 7(9)
C(9)	1.094 9(13)	0.835 1(7)	0.049 3(9)
C(10)	1.029 5(12)	0.788 3(5)	0.076 7(7)
C(11)	0.936 3(12)	0.799 2(6)	0.119 4(7)
C(12)	0.896 8(14)	0.856 6(6)	0.135 7(8)
C(13)	0.800 3(14)	0.858 3(7)	0.176 4(9)
C(14)	0.758 5(14)	0.808 3(7)	0.200 8(9)
C(15)	0.799 6(12)	0.752 7(7)	0.185 9(7)
C(16)	0.755 0(12)	0.695 5(6)	0.209 7(8)
C(17)	0.663 3(12)	0.692 2(9)	0.253 5(7)
C(18)	0.625 1(13)	0.638 4(10)	0.271 2(9)
C(19)	0.679 1(12)	0.585 9(9)	0.247 5(8)
C(20)	0.771 1(12)	0.595 0(7)	0.206 8(8)
C(21)	0.878 4(11)	0.598 5(6)	−0.135 2(7)
C(22)	0.974 4(12)	0.587 7(6)	−0.174 2(8)
C(23)	1.040 1(12)	0.634 7(7)	−0.191 0(8)
C(24)	1.010 1(12)	0.692 1(7)	−0.170 2(7)
C(25)	0.913 5(11)	0.699 9(6)	−0.130 6(6)
C(26)	0.878 3(10)	0.759 1(6)	−0.105 0(6)
C(27)	0.924 2(12)	0.813 9(6)	−0.124 6(7)
C(28)	0.879 4(13)	0.867 2(6)	−0.099 5(8)
C(29)	0.791 1(12)	0.866 1(6)	−0.055 8(8)
C(30)	0.746 4(11)	0.810 0(5)	−0.039 0(7)
C(31)	0.651 1(11)	0.801 0(5)	0.004 8(7)
C(32)	0.589 7(12)	0.848 5(6)	0.031 1(8)
C(33)	0.502 4(12)	0.836 6(7)	0.074 6(9)
C(34)	0.476 6(11)	0.778 2(6)	0.088 8(8)
C(35)	0.539 2(10)	0.731 0(6)	0.060 2(7)
C(36)	0.517 5(10)	0.666 8(5)	0.070 0(6)
C(37)	0.436 9(11)	0.645 1(6)	0.110 9(7)
C(38)	0.425 3(12)	0.583 6(7)	0.119 9(7)
C(39)	0.498 6(12)	0.545 5(6)	0.086 7(7)
C(40)	0.574 5(11)	0.572 8(6)	0.045 7(7)
O(11)	0.270 1(10)	0.754 0(6)	0.216 3(6)
O(12)	0.619 5(10)	0.240 5(6)	0.140 4(6)
O(13)	0.291 4(10)	0.880 4(6)	0.218 2(7)
O(14)	0.630 7(15)	0.991 7(6)	0.209 9(7)
O(15)	0.636 1(13)	0.116 4(7)	0.134 1(9)
O(16)	0.265(3)	0.972 1(8)	0.095 7(16)
O(17)	0.882(4)	0.006 9(9)	0.096 8(16)
O(18)	0.500(3)	0.016 0(11)	0.088 0(15)
O(19)	0	0	0

Table 4 Non-hydrogen atomic coordinates with e.s.d.s for $[\{FeL(Cl)\}_2(\mu\text{-}O)]$

Atom	*x*	*y*	*z*
Fe	0.564 20(9)	0	0.378 96(13)
Cl(1)	0.696 14(16)	0	0.306 25(24)
O(1)	$\frac{1}{2}$	0	$\frac{1}{2}$
N(1)	0.601 0(3)	0.149 1(4)	0.443 2(5)
N(2)	0.490 0(3)	0.092 8(4)	0.228 6(5)
C(1)	0.657 2(4)	0.171 8(5)	0.559 1(7)
C(2)	0.674 7(5)	0.266 9(6)	0.599 7(8)
C(3)	0.634 0(6)	0.340 0(6)	0.519 2(9)
C(4)	0.576 4(5)	0.317 2(5)	0.400 7(8)
C(5)	0.560 2(4)	0.222 3(5)	0.364 8(7)
C(6)	0.497 8(4)	0.188 4(5)	0.242 5(7)
C(7)	0.449 1(5)	0.250 7(5)	0.146 7(7)
C(8)	0.391 4(5)	0.210 7(6)	0.036 2(7)
C(9)	0.383 5(5)	0.111 7(6)	0.023 6(7)
C(10)	0.433 9(4)	0.053 7(4)	0.121 8(7)
Cl(2)	0.170 2(3)	0	0.136 0(4)
O(2)	0.226 1(15)	0	0.242 8(17)
O(3)	0.192 2(10)	0	0.019 8(20)
O(4)	0.130 8(12)	0.072 7(10)	0.130 6(13)
O(5)	0.933 3(9)	0	0.224 4(10)

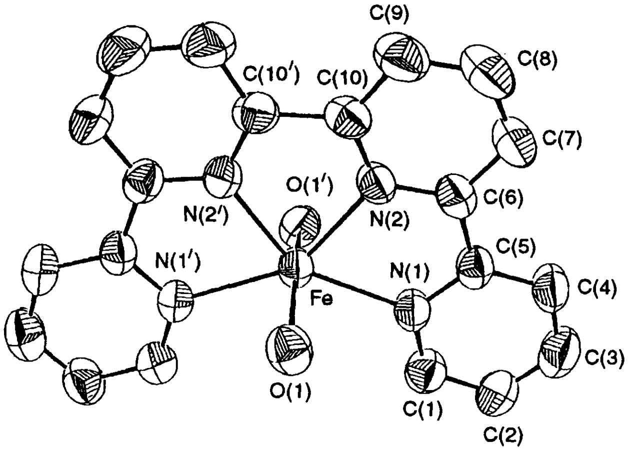

Fig. 1 Perspective view of $[FeL(OH_2)_2]^{2+}$ **1**; primed atoms are generated by a two-fold symmetry axis

product, the crystal structure of which has been determined,[11] which slowly converts to $[\{FeL(Cl)_2\}(\mu\text{-}O)]^{2+}$ **3** in acetonitrile–ethanol solution.

The first unequivocal evidence for the tetradentate co-ordination mode of L was the crystal-structure analysis of $[CoL(OH_2)(SO_3)]NO_3 \cdot H_2O$,[12] followed by characterization of analogous complexes of copper(II),[13] nickel(II),[3a] chromium(III),[3b] palladium(II),[3c] platinum(II),[4a] rhenium(V),[4b] tungsten(IV),[4c] ruthenium(II)[4d] and manganese(II).[4e] The molecular structure of $[FeL(OH_2)_2]^{2+}$ is shown in Fig. 1. It contains two mirror planes probably because of the coplanarity of the quaterpyridine ligand. The two axial H_2O ligands are at a skew angle, pointing towards the N(1)–N(1′) axis between the two terminal pyridyl groups, leading to a O–Fe–O angle of 162.3(2)°. The $Fe-OH_2$ distance of 2.141(5) Å is normal and is comparable to the average value of 2.123(6) Å observed in the high-spin complex $[Fe(H_2O)_6]^{2+}$.[14]

A perspective view of **2** is shown in Fig. 2. The structure features an interesting and rare example of an Fe^{II} complex with a *O,O′*-co-odinating $[ClO_4]^-$ ion. Iron complexes containing singly bound perchlorate ligands are not uncommon and have

Table 5 Selected bond lengths (Å) and angles (°) for the iron complexes

Complex **1**							
Fe–O	2.141(5)	Fe–N(1)	2.198(5)	Fe–N(2)	2.138(5)		
C(5)–C(6)	1.46(1)	C(10)–C(10′)	1.49(1)				
O(1)–Fe–O(1′)	162.3(2)	N(1)–Fe–N(1′)	138.6(2)	N(1)–Fe–N(2)	74.1(2)	N(1)–Fe–O(1)	97.0(2)
N(1)–Fe–N(2′)	147.3(2)	N(1)–Fe–O(1)	86.3(2)	N(1)–Fe–O(1′)	87.5(2)	N(2)–Fe–O(1′)	97.2(2)
N(1)–C(5)–C(6)	115.9(5)	N(2)–C(10)–C(10)	113.3(6)				
Complex **2**							
Fe(1)–O	1.797(8)	Fe(1)–O(1)	2.16(1)	Fe(1)–O(2)	2.14(1)		
Fe(1)–N(1)	2.31(1)	Fe(1)–N(2)	2.21(1)	Fe(1)–N(3)	2.20(1)	Fe(1)–N(4)	2.29(1)
Fe(2)–O	1.785(8)	Fe(2)–O(5)	2.15(1)	Fe(2)–O(6)	2.18(1)		
Fe(2)–N(5)	2.30(2)	Fe(2)–N(6)	2.20(2)	Fe(2)–N(7)	2.24(2)	Fe(2)–N(8)	2.25(2)
C(5)–C(6)	1.51(2)	C(10)–C(11)	1.42(2)	C(15)–C(16)	1.45(2)		
C(25)–C(26)	1.46(2)	C(30)–C(31)	1.45(2)	C(35)–C(36)	1.45(2)		
Fe(1)–O–Fe(2)	155.2(4)	O–Fe(1)–N(1)	90.5(4)	O–Fe(1)–N(2)	100.2(4)		
O–Fe(1)–N(3)	96.1(4)	O–Fe(1)–N(4)	86.0(4)				
N(1)–Fe(1)–N(2)	70.1(3)	N(1)–Fe(1)–N(3)	140.8(4)				
N(1)–Fe(1)–N(4)	148.3(4)	N(2)–Fe(1)–N(3)	70.7(4)	N(2)–Fe(1)–N(4)	141.5(4)	N(3)–Fe(1)–N(4)	70.8(4)
O–Fe(2)–N(5)	86.1(4)	O–Fe(2)–N(6)	99.5(3)	O–Fe(2)–N(7)	103.3(4)	O–Fe(2)–N(8)	88.1(4)
N(5)–Fe(2)–N(6)	71.2(3)	N(5)–Fe(2)–N(7)	141.7(4)	N(6)–Fe(2)–N(8)	140.2(3)	N(7)–Fe(2)–N(8)	69.6(3)
N(5)–Fe(2)–N(8)	148.6(3)	N(6)–Fe(2)–N(7)	70.7(3)				
N(1)–C(5)–C(6)	112.5(10)	N(2)–C(10)–C(11)	117.0(11)	N(3)–C(15)–C(16)	115.9(11)	N(7)–C(35)–C(36)	115.5(10)
N(4)–C(16)–C(15)	113.7(12)	N(5)–C(25)–C(26)	116.9(10)	N(6)–C(26)–C(25)	114.6(10)	N(8)–C(36)–C(35)	113.1(10)
Complex **3**							
Fe–O	1.779(1)	Fe–Cl	2.348(3)	Fe–N(1)	2.191(5)	Fe–N(2)	2.129(5)
C(5)–C(6)	1.48(1)	C(10)–C(10′)	1.48(1)				
O–Fe–Cl	154.95(9)	Fe–O–Fe′	180.0	N(1)–Fe–N(1′)	139.0(2)	N(1)–Fe–N(2)	85.0(1)
N(2)–Fe–N(2)	73.7(2)	N(1)–Fe–O	86.3(1)	N(2)–Fe–O	102.6(1)	N(1)–Fe–Cl	85.0(1)
N(2)–Fe–Cl	97.4(2)	N(1)–C(5)–C(6)	113.4(6)	N(2)–C(10)–C(10′)	113.5(6)		

Table 6 Energy and composition of the near-frontier orbitals of the cation of complex **2**

	Composition (%)			
Energy/eV	2Fe	O	$2ClO_4$	2L
1.2625	0.34	0.06	0.06	99.54
1.1537	0.47	0.19	0.11	99.23
1.0694	0.71	0.12	0.19	98.98
1.0040	0.74	0.39	0.25	98.62
0.8789	0.31	0.10	0.05	99.54
0.5306 (LUMO)	0.57	0.38	0.18	98.87
−7.3385 (HOMO)	51.68	42.89	3.07	2.36
−7.4691 (NHOMO)	49.44	45.61	1.03	3.92
−8.4814	78.06	12.52	5.14	4.28
−8.7589	84.69	0.55	5.13	9.63
−8.9222	81.74	8.11	1.73	8.42
−9.5453	96.77	0.03	1.00	2.20
−11.2731	39.68	48.19	6.24	5.88
−11.4772	44.14	39.13	2.94	13.79
−11.6241	42.11	39.25	10.61	8.02
−12.0976	2.87	2.13	93.66	1.34
−12.1982	1.99	2.08	94.77	1.16
−12.3098	0.90	0.46	1.20	97.44

Table 7 Energy and composition of the near-frontier orbitals of the cation of complex **3**

	Composition (%)			
Energy/eV	2Fe	O	2Cl	2L
0.7597	0.26	0.00	0.02	99.72
0.6916	0.39	0.00	0.28	99.33
0.6508	1.83	0.00	0.21	97.96
0.6263	0.16	0.03	0.02	99.79
0.2862	1.86	0.02	1.28	96.84
0.0359 (LUMO)	13.25	0.28	3.37	83.10
−4.5653 (HOMO)	77.97	2.20	18.34	1.49
−4.9381 (NHOMO)	72.30	1.79	24.16	1.75
−10.0264	16.55	12.54	68.50	2.41
−10.4536	23.05	8.42	66.50	2.03
−12.6603	9.53	8.07	31.55	50.85
−12.6902	4.42	1.87	71.42	22.29
−12.7637	4.00	1.27	70.45	24.28
−12.7800	4.65	3.24	35.12	56.99
−12.9324	14.38	21.70	37.04	26.88
−13.0930	10.42	16.00	24.18	49.41
−13.0984	3.56	4.00	10.24	82.11
−13.3623	13.34	13.87	32.43	40.36

been reviewed.[15] Here, the iron atom is seven-co-ordinate and this is quite different from the co-ordination in **1** and in **3**. The co-ordinated Cl–O distances, ranging from 1.458(9) to 1.523(10) Å, are longer than all the unco-ordinated distances in **2** and **3** which may suggest the weakening of the Cl–O bond through co-ordination of ClO_4^- to Fe^{II}.

Fig. 3 shows a perspective view of the complex cation of **3**, which is unique among other iron complexes having α-diimine ligands. For the $[\{Fe(phen)_2(OH_2)\}_2O]^{4+}$,[16] $[\{Fe(phen)_2Cl\}_2O]^{2+}$ [17] and $[\{Fe(phen)(OH_2)_3\}_2O]^{4+}$ [18] (phen = 1,10-phenanthroline) complexes studied previously, the two α-diimine moieties are *cis* to each other and the Fe_2O unit (155–162°) is bent, whereas in **3**, the two quaterpyridine planes are parallel and the Fe–O–Fe angle is 180°. Iron(III) complexes bearing a linear Fe–O–Fe unit have been reported previously: the observed Fe–O distance of 1.779(1) Å in **3** is comparable to that of 1.772–1.773 in $[\{Fe(H_2O)_2(L')\}_2O]$ (L′ = 4-chloro-2,6-pyridinedicarboxylate),[19] and of 1.763 Å in $[(FeL'')_2O]$ (H_2L'' = 5,10,15,20-tetraphenylporphyrin).[20] The two quaterpyridines in **3** are coplanar and are separated by about 3.56 Å.

Complexes **1** and **2** are diamagnetic. Complex **3** is paramagnetic with a measured μ_{eff} of 1.75 μ_B per iron centre.

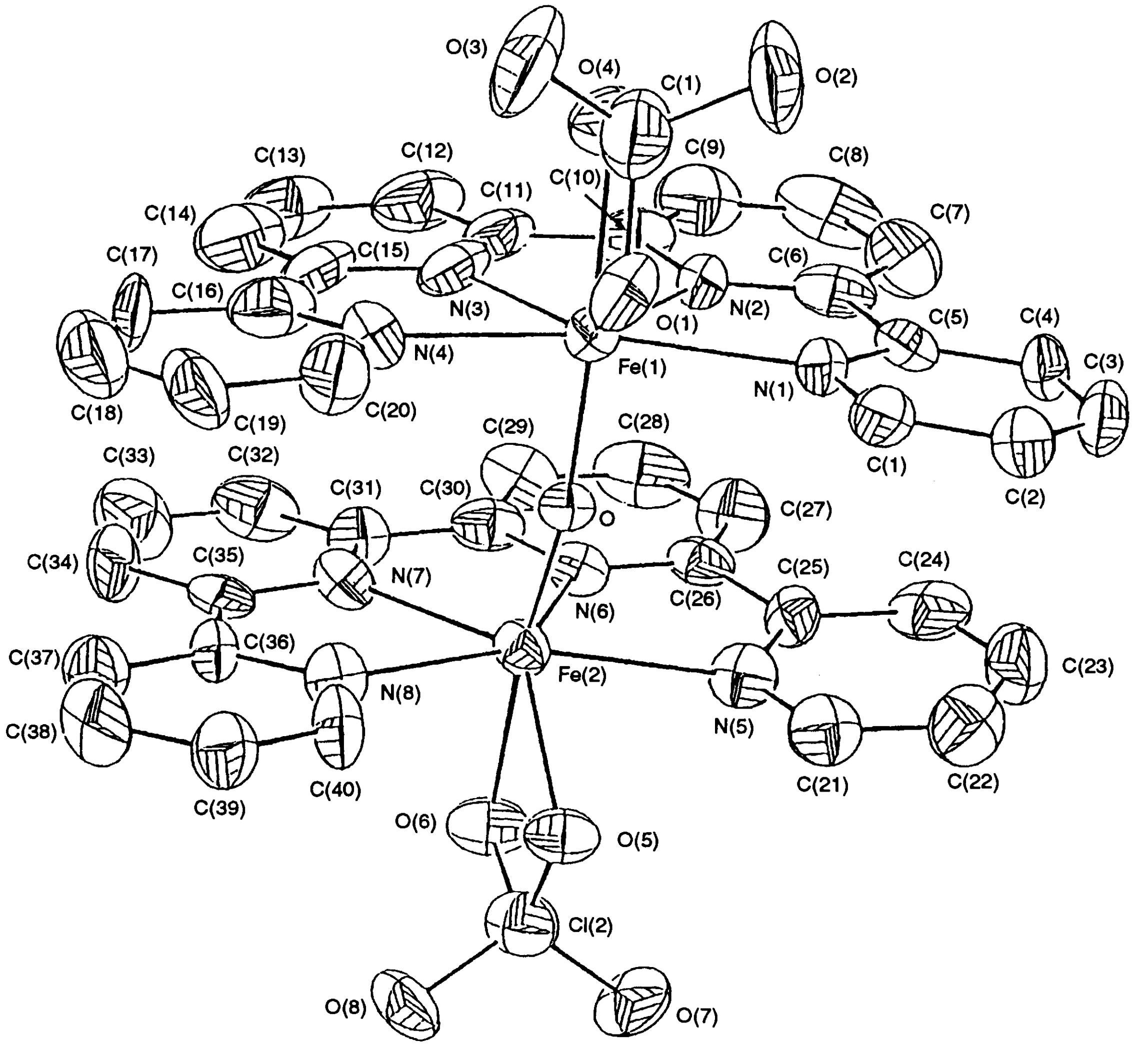

Fig. 2 Perspective view of [{FeL(ClO$_4$)}$_2$(μ-O)] **2**

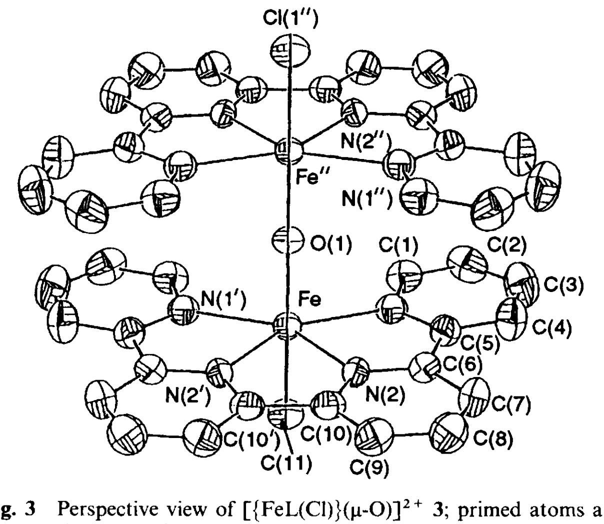

Fig. 3 Perspective view of [{FeL(Cl)}(μ-O)]$^{2+}$ **3**; primed atoms are generated by a two-fold mirror plane

This is in line with the results of the calculations described below, which indicates an open-shell ($S = 1$) ground state. Molecular-orbital calculations on **2** and **3** have been undertaken and the energies and composition of the near-frontier orbitals are listed in Tables 6 and 7 respectively.

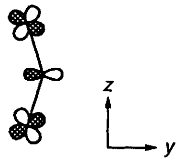

Fig. 4 The HOMO of the complex cation **2**

The highest occupied molecular orbital (HOMO) of **2** is shown in Fig. 4. In the HOMO, however, the oxygen p_y orbital is displaced from the Fe–Fe axis. This results in a decrease in the antibonding interaction between the O(p_y) and two Fe(d_{yz}) orbitals. As a result, the two Fe–L planes are tilted. In the next HOMO (NHOMO), the bending of Fe–O–Fe has a small influence in the orbital energy as the two d_{xz}(Fe) and p_x(O) orbitals are not in the same plane. The LUMO is mainly comprised of the π* orbital of L. Thus, the intense low energy absorption band in the visible region can be ascribed to metal-to-ligand charge-transfer transitions.

The total electron energy of **3** was calculated for both the open-($S = 1$) and closed-shell ($S = 0$) states. The results showed that the former is more stable than the latter by 49.3 kcal mol^{-1} and that the HOMO and NHOMO have comparable energies. This is in accord with the experimental finding that complex **3** has two unpaired electrons The interaction between Fe(d_{xz},d_{yz}) and Cl(p_x,p_y) orbitals is dominant in both the HOMO and NHOMO, and the two unpaired electrons are localized in the Fe–Cl bonding orbitals. The LUMO is mainly composed of the π^* orbital of L.

Acknowledgements

We acknowledge support from The Hong Kong Research Grants Council and The University of Hong Kong. C.-W. C. is thankful to the award of a Hung Hing-Ying Scholarship (1992–93) administrated by The University of Hong Kong.

References

1 V. Balzani, F. Bolleta, T. Gandolfi and M. Maestri, *Top. Curr. Chem.*, 1978, **75**, 1.
2 E. C. Constable, *Adv. Inorg. Chem.*, 1986, **30**, 69; *Prog. Inorg. Chem.*, 1994, **42**, 67.
3 (*a*) E. C. Constable, S. M. Elder, J. Healy and D. A. Tocher, *J. Chem. Soc., Dalton Trans.*, 1990, 1669; (b) E. C. Constable, S. M. Elder and D. A. Tocher, *Polyhedron*, 1992, **11**, 1337; (*c*) E. C. Constable, S. M. Elder, J. Healy and M. D. Ward, *J. Am. Chem. Soc.*, 1990, **112**, 4590.
4 (*a*) C. W. Chan, C. M. Che, M. C. Cheng and Y. Wang, *Inorg. Chem.*, 1992, **31**, 4874, (*b*) C. M. Che, Y. P. Wang, K. S. Yeung, K. Y. Wong and S. M. Peng, *J. Chem. Soc., Dalton Trans.*, 1992, 2675; (*c*) S. M. Yang, K. K. Cheung and C. M. Che, *J. Chem. Soc., Dalton Trans.*, 1993, 3515; (*d*) C. W. Chan, T. F. Lai and C. M. Che, *J. Chem. Soc., Dalton Trans.*, 1994, 895; (*e*) C. W. Chan, C. M. Che and S. M. Peng, *Polyhedron*, 1993, **12**, 2169.
5 M. Branca, B. Pispisa and C. Aurisicchio, *J. Chem. Soc., Dalton Trans.*, 1976, 1543; M. Cerdonio, F. Mogno, B. Pispisa, G. L. Romani and S. Vitale, *Inorg. Chem.*, 1977, **16**, 400; B. Pispisa, M. Barteri and M. Farinella, *Inorg. Chem.*, 1983, **22**, 3166; B. Pispisa, A. Palleschi and G. Paradossi, *J. Mol. Catal.*, 1987, **42**, 269.
6 D. H. R. Barton and D. Doller, *Acc. Chem. Res.*, 1992, **25**, 504; T. Kojima, R. A. Leising, S. Yan and L. Que, *J. Am. Chem. Soc.*, 1993, **115**, 11328.
7 NRCVAX, E. J. Cabe, Y. Le Page, J. P. Charland, F. L. Lee and P. S. White, *J. Appl. Crystallogr.*, 1989, **22**, 384.
8 A. Earnshaw, *Magnetochemistry*, Academic Press, New York, 1969.
9 G. C. Allen and D. W. Clark, *J. Chem. Soc. A.*, 1970, 2668.
10 J. A. Pople and D. L. Beveridge, *Approximate Molecular Orbital Theory*, McGraw-Hill, New York, 1970.
11 C. Y. Lee and C. M. Che, unpublished work.
12 E. N. Maslen, C. L. Raston and A. H. White, *J. Chem. Soc., Dalton Trans.*, 1975, 323.
13 W. Henke, S. Kremer and D. Reinen, *Z. Anorg. Allg. Chem.*, 1982, **491**, 124.
14 J. Strouse, S. W. Layten and C. E. Strouse, *J. Am. Chem. Soc.*, 1977, **99**, 562.
15 N. M. N. Gowda, S. B. Naikar and G. K. N. Reddy, *Adv. Inorg. Chem. Radiochem.*, 1984, **28**, 255.
16 J. E. Plowman, T. M. Loehr, C. K. Schauer and O. P. Anderson, *Inorg. Chem.*, 1984, **23**, 3553.
17 P. C. Healy, B. W. Skelton and A. H. White, *Aust. J. Chem.*, 1983, **36**, 2057.
18 P. C. Healy, J. M. Patrick and A. H. White, *Aust. J. Chem.*, 1984, **37**, 1405.
19 C. C. Ou, R. G. Wollmann, D. N. Hendrickson, J. A. Potenza and H. J. Schugar, *J. Am. Chem. Soc.*, 1978, **100**, 4717.
20 A. B. Hoffman, D. M. Collins, V. M. Day, E. B. Fleischer, T. S. Srivastava and J. L. Hoard, *J. Am. Chem. Soc.*, 1972, **94**, 3620.

Received 31*st January* 1995; *Paper* 5/00573F